TPPP/p25 promotes tubulin assemblies and blocks mitotic spindle formation

L. Tirián*, E. Hlavanda†, J. Oláh†, I. Horváth†, F. Orosz†, B. Szabó‡, J. Kovács§, J. Szabad*, and J. Ovádi†¶

*Department of Biology, Faculty of Medicine, University of Szeged, H-6720, Szeged, Hungary; Departments of ‡Biological Physics and §Zoology, Eötvös Loránd University, Budapest, H-1117, Hungary; and †Institute of Enzymology, Biological Research Center, Hungarian Academy of Sciences, Budapest, H-1518, Hungary

Communicated by Tibor Farkas, Hungarian Academy of Sciences, Szeged, Hungary, October 1, 2003 (received for review July 1, 2003)

Recently, we isolated from bovine brain a protein, TPPP/p25 and identified as p25, a brain-specific protein that induced aberrant tubulin assemblies. The primary sequence of this protein differs from that of other proteins identified so far; however, it shows high homology with p25-like hypothetical proteins sought via BLAST. Here, we characterized the binding of TPPP/p25 to tubulin by means of surface plasmon resonance; the kinetic parameters are as follows: k_{on}, 2.4 × 10^4 $M^{-1}s^{-1}$; k_{off}, 5.4 × 10^{-3} s^{-1}; and K_d, 2.3 × 10^{-7} M. This protein at substoichometric concentration promotes the polymerization of tubulin into double-walled tubules and polymorphic aggregates or bundles paclitaxel-stabilized microtubules as judged by quantitative data of electron and atomic force microscopies. Injection of bovine TPPP/p25 into cleavage *Drosophila* embryos expressing tubulin–GFP fusion protein reveals that TPPP/p25 inhibits mitotic spindle assembly and nuclear envelope breakdown without affecting other cellular events like centrosome replication and separation, microtubule nucleation by the centrosomes, and nuclear growth. GTP counteracts TPPP/p25 both *in vitro* and *in vivo*.

The cytoplasm of eukaryotic cells contains an elaborate network of cytoskeletal elements, consisting of actin and intermediate filaments and microtubules (MTs) engaged in a variety of cell functions, such as the extension and guidance of neurons or the formation of mitotic spindles required for chromosomal segregation. The polymerization dynamics of tubulin to MTs is under strict control (1). Numerous proteins have been reported to interact with the MTs as positive regulators of MT assembly (microtubule-associated proteins), either by promoting the polymerization of tubulin or by stabilizing MTs (1, 2). Only a few proteins are known to act as destabilizers, such as Op18/stathmin, katanin, and some kinesin-like proteins (1, 2). We have reported recently that the M1 isoform of pyruvate kinase and *Dictyostelium discoideum* phosphofructokinase inhibit tubulin polymerization or promote disassembly of the MTs to thread-like oligomers *in vitro* (3–5).

Recently, from bovine brain, we isolated and identified a protein that we denoted TPPP/p25 (6), which corresponded to p25 (NCBI accession no. 2498194). This protein is a heat stable, cationic protein that induces polymerization of tubulin into unusual forms or bundling of paclitaxel-stabilized MT. The TPPP/p25 protein was partially copurified with a tau kinase (7). The bovine TPPP/p25-coding gene has been cloned (8), and recently the human homologue of TPPP/p25 was cloned and mapped to the p15.3 region of chromosome 5. The identity between the bovine and human TPPP/p25 proteins is 90% (9). This protein was also described as p24, a heat-resistant glycogen synthase kinase-3 inhibitor (10). It is important to note that TPPP/p25 differs completely from the extensively characterized protein p25, which is a truncated form of p35 that deregulates cyclin-dependent kinase-5 activity by causing prolonged activation and mislocalization of the kinase (11). To avoid further confusion about the name of this protein, we suggest using the term TPPP (*t*ubulin *p*olimerization-*p*romoting *p*rotein), which highlights its characteristic action on tubulin (see ref. 6 and below).

In this article, we characterize the binding of the isolated TPPP/p25 protein to tubulin immobilized on a BIAcore (Uppsala, Sweden) chip, demonstrate the modulating effect of GTP on the TPPP/p25-induced alterations, and present electron microscopic as well as atomic microscopic images for the TPPP/p25-induced ultrastructural alteration in MT structures. To study the effect of TPPP/p25 on microtubular system *in vivo*, we injected TPP/p25 into *Drosophila* cleavage embryos expressing GFP-fusion tubulin. The *Drosophila* embryo was chosen as a model organism because it is characterized by waves of synchronized spindle assemblies and nuclear divisions. We have found that TPPP/p25 injection inhibits mitotic spindle assembly without affecting other cellular events like centrosome replication and segregation, nucleation of MTs by the centrosomes, and nuclear growth.

Experimental Procedures

Chemicals. EGTA, GDP, GTP, Mes, Tris, and paclitaxel were purchased from Sigma. Biotin-XX SSE (Cat. no. B6352) was from Molecular Probes. Streptavidin-coated sensor chips were bought from BIAcore. All other chemicals were reagent grade commercial preparations. Solutions were prepared by using Millipore's Milli-Q ultra-pure water.

Protein Determination. Protein concentration was measured by the Bradford method (12) by using the Bio-Rad Protein Assay Kit.

Tubulin and MT Preparation. Microtubule-associated protein (MAP)-depleted tubulin was purified from bovine brain by the method of Na and Timasheff (13) and stored in 10 mM phosphate buffer (pH 7.0), containing 1 M sucrose, 0.5 mM $MgCl_2$, and 0.1 mM GTP at −80°C. Purified tubulin showed no contamination with MAPs on overloaded SDS/PAGE. Before use, stored tubulin was dialyzed against 50 mM Mes buffer (pH 6.8) at 4°C for 3 h and then centrifuged at 100,000 × *g* for 20 min at 4°C. MTs were assembled by adding 20 μM paclitaxel to 10 mg/ml tubulin, followed by incubation for 30 min at 37°C.

TPPP/p25 Preparation. The protein was isolated from bovine brain as described (6). Briefly, the homogenized bovine brain was heat-treated at 90°C, and the concentrated supernatant was chromatographed on anion exchange resin and then the unbound fraction on cation exchange resin. The salt-eluted and concentrated fractions were applied to a cation exchange HPLC system, and the fraction eluted above 0.5 M salt concentration

Abbreviations: TPPP/p25, tubulin polymerization promoting protein, MT, microtubule; SPR, surface plasmon resonance; AFM, atomic force microscopy; TEM, transmission electron microscopy; NE, nuclear envelope.

¶To whom correspondence should be addressed at: Institute of Enzymology, Biological Research Center, Hungarian Academy of Sciences, 1113 Budapest, Karolina út 29, Hungary. E-mail: ovadi@enzim.hu.

www.pnas.org/cgi/doi/10.1073/pnas.2436331100

was dialyzed, concentrated, and used as TPPP/p25 protein. This fraction showed no other protein band on SDS/PAGE. It was stored at −80°C.

Surface Plasmon Resonance (SPR) Measurement. The binding kinetics of TPPP/p25 to tubulin were monitored in real-time with a BIAcore X instrument (BIAcore). Tubulin at a concentration of 10 mg/ml was biotinylated with a sulfosuccinimidyl ester derivative of biotin, and the biotinylated tubulin at a concentration of 0.5 μM was immobilized onto a streptavidin-coated sensor chip (Sensor Chip SA, product code BR-1000-32, BIAcore) as described (14). All experiments were performed at 25°C. Sensorgrams were recorded at a flow rate of 5 μl/min for 3 min at three different concentrations of TPPP/p25. Dissociation and association rate constants were calculated by a linearization method based on Eq. **1**:

$$\ln \frac{dR}{dt} = \ln(k_{on}CR_{max}) - (k_{on}C + k_{off})t, \qquad [1]$$

where dR/dt is the rate of change of SPR signal, C is the concentration of analyte (TPPP/p25), R_{max} is the maximum analyte-binding capacity in response units (RU), and R is the SPR signal in RU at time t. The slope of plot of $\ln(dR/dt)$ vs. t is $-(k_{on}C + k_{off})$ as denoted k_{obs}; the tangent of k_{obs} vs. C gives k_{on} (knowledge of R_{max} is not necessary), and the intercept on the ordinate is k_{off}. For the linear fitting, ORIGIN 5.0 software from Microcal (Amherst, MA) was used. The error of determination was <10%.

Polymerization Assays. Tubulin (10 μM) was assembled to MT at 37°C in 50 mM Mes buffer (pH 6.6), containing 2 mM dithioerythritol, 5 mM $MgCl_2$, 1 mM EGTA (polymerization buffer), and KCl in concentrations as indicated. The polymerization was initiated with TPPP/p25 in the absence and presence of GTP or ATP. For turbidity measurements, absorbance was monitored at 350 nm with a Cary 50 spectrophotometer (Varian).

Transmission Electron Microscopy (TEM). MT-containing samples were pelleted by centrifugation, and the pellets were prefixed with 2% glutaraldehyde and 0.2% tannic acid in 0.1 M sodium cacodylate (pH 7.4) for 60 min, and then washed with 0.1 M sodium cacodylate, postfixed with 0.5% OsO_4 in 0.1 M sodium cacodylate, stained *en bloc* with 1% uranyl acetate, dehydrated in graded ethanol, and embedded in Durcupan (Fluka). Thin sections were contrasted with uranyl acetate and lead citrate and examined and photographed in a JEOL CX 100 electron microscope. For negative staining, a drop from the unpelleted samples obtained from the polymerization assay was applied to glow-discharged formvar/carbon-coated copper grids for 30 s. This was followed by staining with a drop of freshly filtered 1% aqueous uranyl acetate for 40 s.

Atomic Force Microscopy (AFM). We used a commercial AFM (TopoMetrix Explorer, Santa Clara, CA) in contact mode with a soft silicon nitride cantilever (Thermomicroscopes, coated sharp microlevers, model no. MSCT-AUHW, with typical force constant 0.03 N/m, 20 nm nominal radius of curvature) at room temperature. Clean 13-mm glass cover slips were coated with poly-L-lysine (Sigma) by placing a drop of 0.1% wt/vol solution on them. After 3 min, we removed the excess polylysine, washed the surface three times with distilled water, and dried it in airflow. We dropped 10 μl of the MT samples on the coated cover slips. Drops were air-dried immediately. Samples were washed with distilled water, and air-dried again. AFM images were scanned in air with a typical frequency of 5 Hz. For quantitative evaluation of length and width distribution of MTs, we used the analyzer software of TopoMetrix. In each case, the number of measurements was at least 10.

Microinjection of TPPP/p25 into Cleavage *Drosophila* Embryos. To visualize the effect of TPPP/p25 in cleavage *Drosophila* embryos, we injected ≈200 pl per egg (≈ 2% total egg volume) from a solution that contained 160 μM purified TPPP/p25 protein, alone or together with 10 mM GTP, into stage 10 cleavage embryos expressing tubulin–GFP (15). After injections, fate of the injected embryos was followed by time lapse cinematography through the collection of optical sections in a ZEISS LSM410 confocal microscope. The injections were done at 20°C.

Results

TPPP/p25 Is the First Member of a New Protein Family. The bovine and human TPPP/p25 genes have been cloned (8, 9), and very high (90%) identity was found between them (see Fig. 6, which is published as supporting information on the PNAS web site). Very recently their mouse counterpart (XP_138708) was also identified in the NCBI Annotation Project (http://www.ncbi.nlm.nih.gov/LocusLink/LocRpt.cgi?l=238721), and shares 93% and 87% identity with the human and bovine TPPP/p25, respectively. Taking into consideration conservative replacements, the pair-wise similarity of these proteins is higher than 95%.

TPPP/p25 protein does not show homology with other proteins identified so far, but we found homologies at the nucleic acid levels among additional TPPP/p25-like hypothetical proteins sought via BLAST (16). The search results suggest that the bovine TPPP/p25 protein, the only protein isolated and characterized so far, is a member of a new protein family characterized by high homology of C-terminal parts of these proteins.

A subclass of this family has been found in mammals, in which, however, the first 40–42 aa of the N-terminal part of these proteins are missing as compared with the bovine protein. (This initial N-terminal part of TPPP/p25 does not show significant homology with other proteins in the database.) The proteins within the subclass are, however, similar to each other (52–96% identity) and to the C-terminal part of TPPP/p25 (57–81% identity). Therefore, there are at least three if not four genes coding for TPPP/p25-like proteins in mammals. In humans, they are located on the 5th, 14th, and 16th chromosomes (9, 17).

The mammalian TPPP/p25-like proteins share homology with further putative proteins from invertebrate species (Fig. 6). In *Drosophila melanogaster*, *Caenorhabditis elegans*, and *Anopheles gambiae*, organisms with completely sequenced and well-annotated genome, only a single homologous gene is present, and the predicted proteins are composed of 192, 180, and 225 aa, respectively. These gene products are 40–48% identical with each other and with the TPPP/p25-related mammalian proteins. However, if we consider only the last 50 aa of the C-terminal parts of the sequences, then the identity is considerably higher (80%). Although there are several other well-conserved sections in all these proteins, the single motif identified so far is the Rossmann motif, GXGXXG, characteristic for ATP-binding site of proteins (18). Searching for homology in databases, the next TPPP/p25-related putative protein is a thermophilic one (Igr3p; 34% identity with the bovine TPPP/p25 protein), which does not contain the characteristic Rossmann motif, suggesting that it may not belong to the TPPP/p25 protein family.

Quantitative Characterization of TPPP/p25-Tubulin Interaction. In a previous article, we showed that TPPP/p25 purified from bovine brain interacts with microtubules (6). To obtain direct quantitative data on the binding of TPPP/p25 to tubulin, the association and dissociation kinetics of the interaction were followed by SPR measurements. Fig. 1*A* shows typical sensorgrams obtained at 40-nM, 80-nM, and 160-nM TPPP/p25 concentrations

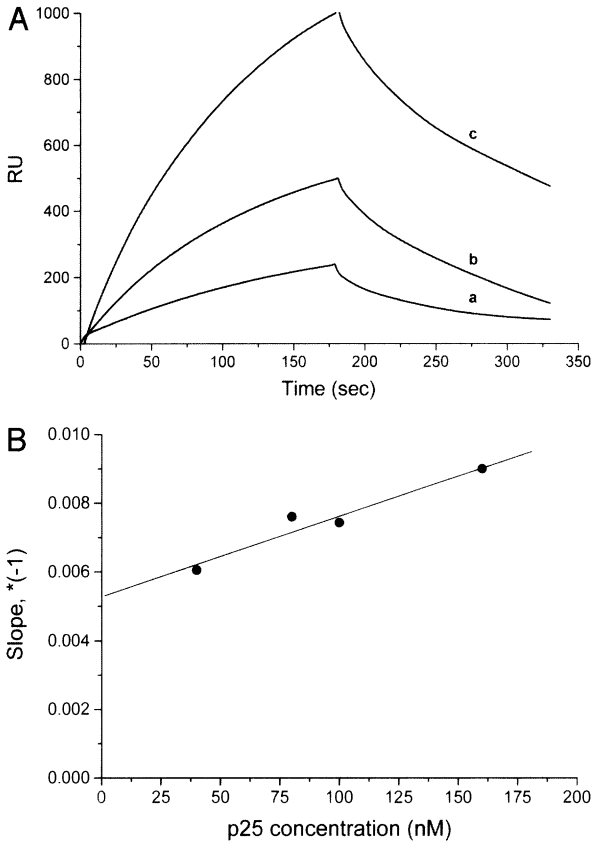

Fig. 1. TPPP/p25-tubulin interaction monitored by SPR. (*A*) TPPP/p25 (a, 40 nM; b, 80 nM; and c, 160 nM) was injected to biotinylated tubulin immobilized on streptavidin covered chip. (*B*) Determination of k_{on} and k_{off} by straight line fitting of the k_{obs} vs. TPPP/p25 concentration graph.

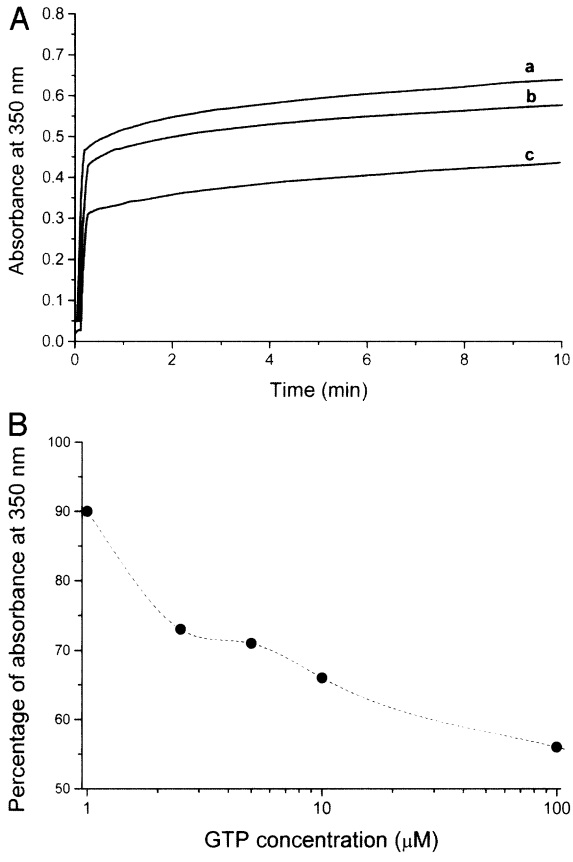

Fig. 2. Effect of GTP on the TPPP/p25-induced tubulin oligomerization as determined by turbidimetry. (*A*) Concentrations of tubulin and TPPP/p25 were 10 μM and 0.6 μM, respectively. GTP concentrations were as follows: a, 0 μM; b, 1 μM; and c, 100 μM. (*B*) Effect of GTP on turbidity of tubulin solution induced by TPPP/p25 at 10 min.

(*C*), when biotinylated tubulin was immobilized onto a streptavidin-coated sensor chip. The kinetic constants, k_{on} and k_{off}, evaluated from the plot of k_{obs} vs. C (compare *Experimental Procedures*) are as follows: k_{on}, 2.4×10^4 $M^{-1} \cdot s^{-1}$; k_{off}, 5.4×10^{-3} s^{-1} (Fig. 1*B*). The dissociation constant $K_d = k_{off}/k_{on}$ is 2.3×10^{-7} M. These data suggest that TPPP/p25 binding to tubulin is tight. Similar binding parameters were obtained for tubulin–tubulin interaction by SPR under similar conditions, as well (14).

GTP Inhibits the TPPP/p25-Induced Tubulin Polymerization. We have previously demonstrated that brain and neuroblastoma but not muscle extract stimulate paclitaxel-assisted tubulin polymerization as followed by turbidimetry (19). The partially purified but especially the isolated TPPP/p25 protein initiates the assembly of microtubule-associated protein-free tubulin even in the absence of paclitaxel. The effect is manifested at substoichiometric TPPP/p25 concentrations (6). Here, we investigated the effect of GTP on the TPPP/p25-induced tubulin assembly. As shown in Fig. 2, the rapid enhancement in the turbidity of 10 μM tubulin caused by 0.6 μM TPPP/p25 is reduced by the addition of GTP in a concentration-dependent manner. These data suggest that TPPP/p25 and GTP interfere with each other for tubulin binding.

AFM and TEM Analysis of TPPP/p25-Induced Tubulin Assemblies. To obtain direct and quantitative data on the structure of assembly products, we used AFM in parallel with TEM. As seen in the images of AFM, the population of normal, paclitaxel-stabilized MTs consists of tens of microns long irregularly arranged single MTs adhered to the polylysine-coated glass surface (Fig. 3*A*). Thin-section electron microscopy of the corresponding resin-embedded samples reveals that the diameter of MTs prepared by the method used here is ≈25 nm (Fig. 3*D*), which is in agreement with our previous data (20). However, in the AFM images, their apparent width is 120 ± 10 nm due to the well known widening effect of the AFM tip.

After addition of TPPP/p25 (0.2–2 μM) to paclitaxel-stabilized MTs, amorphous aggregates and rods with a length of 2,500 ± 1,000 nm and a calculated diameter of 112 ± 23 nm appear on the AFM images of the samples (Fig. 3*B*). Because the rods are about five times wider than the single MTs, we consider them as bundled MTs. Examination of TEM pictures taken from the resin-embedded counterpart of the same samples strengthens this conclusion. They clearly show the presence of bundles of closely aligned MTs (Fig. 3*E*).

AFM examination of samples prepared with addition of TPPP/p25 to tubulin in the absence of paclitaxel also reveals the presence of tubulin aggregates and short rod-like structures (data not shown). The resin-embedded and thin-sectioned counterparts of these samples contain numerous double-walled MTs of ≈40 nm diameter (Fig. 3*C*) as described in our previous study (6). On negatively stained whole-mounts, they appear as single MTs, the walls of which are covered by a row of tightly packed small particles. In some cases, they form small bundles consisting of 2–3 MTs (Fig. 3*F*). Taken together, the AFM and TEM results are in good agreement and confirm the massive effect of the TPPP/p25 on the polymerization of tubulin and prove that TPPP/p25 induces the formation of aberrant tubulin assemblies under the conditions used here.

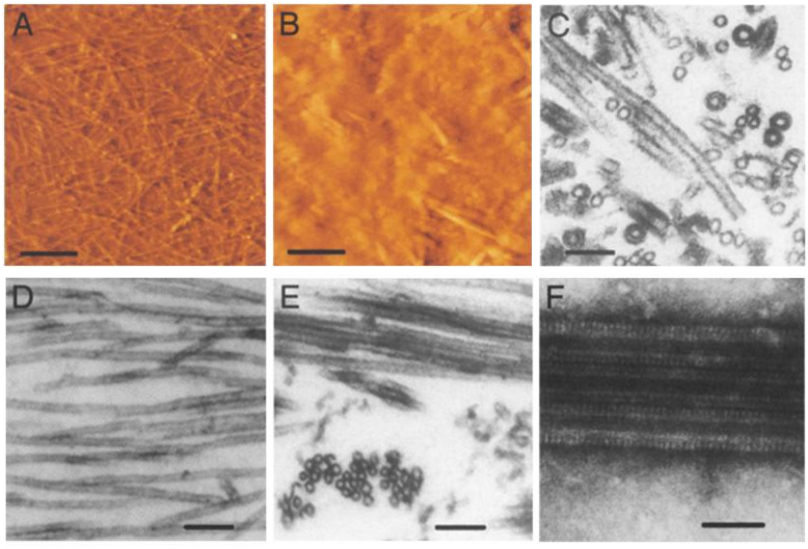

Fig. 3. Images of MTs by AFM (*A* and *B*) and TEM (*C–F*). Samples were prepared without (*A* and *D*) and with addition of TPPP/p25 (*B*, *C*, *E*, and *F*). Loosely arranged single MTs are seen in *A* and *D*. TPPP/p25 induces bundling of paclitaxel-stabilized MTs (*B* and *E*). When added to tubulin in the absence of paclitaxel, TPPP/p25 induces the formation of tubulin aggregates and double-walled MTs (*C*), which appear as thick MTs covered by periodic rows of particles on negatively stained whole mounts (*F*). (Bars = 2 μm in *A* and *B*; 100 nm in *C*, *D*, and *E*; and 50 nm in *F*.)

TPPP/p25 Injection into Cleavage *Drosophila* Expressing Tubulin–GFP Fusion Protein. To study the *in vivo* effect of TPPP, we injected bovine-derived and purified TPPP into cleavage *Drosophila* embryos expressing tubulin–GFP fusion protein. Microinjection of proteins into cleavage embryos has been found to be a powerful method to study the functions of proteins that affect cell cycle progression because the synchronized nuclear divisions 9–14 commence at the surface of the shared egg cytoplasm, allowing visualization of the effects of the injected protein on several nuclei and spindles.

We injected ≈200 pl (≈2% egg volume) 160 μM TPPP/p25 protein into the embryos to reach (after the diffusion of the protein) the concentration of TPPP/p25 that exerts clear effects on *in vitro* tubulin oligomerization assays. In the first set of experiments, the effect of TPPP/p25 on the mitotic spindle was investigated. The purified TPPP/p25 protein was injected into the posterior pole of tubulin–GFP-expressing *Drosophila* cleavage embryos at the anaphase of cleavage division 10. The injected protein has no immediate effect on the anaphase spindles because chromosomes segregate and nuclei form normally around the site of injection (Fig. 4*A*). The nuclei grow and are intact in the next interphase because nuclei appear as dark areas, showing that tubulin-GFP cannot enter the nuclei. On the onset of the next cleavage mitosis (Fig. 4*B*), mitotic spindles are absent around the site of injection whereas normal spindles form in the anterior (control) part of the embryo that are probably free from TPPP/p25. The failure of mitotic spindle formation in the presence of TPPP/p25 inhibits breakdown of the nuclear envelope (NE) as indicated by the exclusion of tubulin-GFP from nuclei at the site of TPPP/p25 action during the whole mitotic wave. TPPP/p25 does not inhibit replication or MT-dependent segregation of centrosomes during the following interphase: several large nuclei that failed to divide are surrounded by four normally segregated centrosomes, and many centrosomes detach from the NE (data not shown). Note that TPPP/p25 does not inhibit nucleation of MTs by the centrosomes: the centrosomes are visible because they nucleate seemingly normal MT asters.

In the next mitotic wave, as a consequence of further diffusion of TPPP/p25 to the middle part of the embryo, mitotic spindles form only in the anterior part, and nuclei remain intact in the middle and posterior part of the embryo (Fig. 4*D*). Because nuclear growth and the division of centrosomes is not affected again, there are three types of nuclei in the third interphase after TPPP/p25 injection (Fig. 4*E*). (*i*) Nuclei at the site of injection failed to divide twice, and are the largest ones surrounded by up

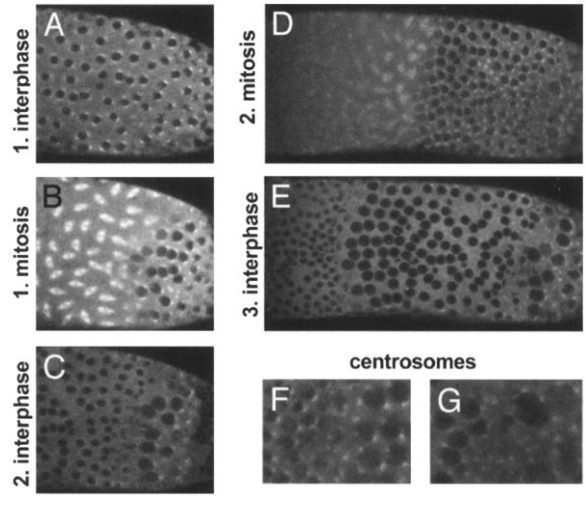

Fig. 4. TPPP/p25 inhibits mitotic spindle formation and NE breakdown in *Drosophila* cleavage embryos. TPPP/p25 was injected into the posterior pole (*Right*) of tubulin–GFP-expressing cleavage *Drosophila* embryos. In the first interphase after injection nuclei seem normal (*A*). During the next mitotic wave mitotic spindles do not form and NE does not break down around the site of injection (*B*). After breakdown of the mitotic spindles, nuclei form normally and, as a consequence, nuclei with two different sizes from anterior and middle parts of the embryo contain nuclei of normal size, but the nuclei in the vicinity of injection site are larger, because they fail to divide but enlarge constantly (*C*). During the second mitotic wave after TPPP/p25 injection, mitotic spindles form only in the anterior part of the embryo (*D*). After the mitotic wave nuclei form again, the embryo contains three types of nuclei: (*i*) very large nuclei surrounded by up to eight centrosomes (for centrosomes see *G*) in the vicinity of injection, (*ii*) large nuclei surrounded by up to four centrosomes (see *F* and *G*) where mitotic spindles formed only once after TPPP/p25 injection, and (*iii*) nuclei of normal size at TPPP/p25-unaffected regions (*E*). (*F* and *G*) Enlarged representative areas from *E* in a different focal plane.

to eight centrosomes (Fig. 4*G*). (*ii*) Nuclei in the middle section are also larger than normal because they divided only once and are surrounded by up to four centrosomes (Fig. 4 *F* and *G*). The TPPP/p25-affected region of the embryo contains several free centrosomes detached from the nuclei. (*iii*) The anterior part of the embryo contains normal-sized nuclei with two centrosomes (Fig. 4*F*). Results of the tubulin–GFP injection experiments revealed that (*i*) TPPP/p25 inhibits formation of mitotic spindles but (*ii*) does not interfere with centrosome duplication and separation and the MT nucleation by the centrosomes. The experiments also showed that, unlike in mammalian cell cultures where NEs, although slower than normally, break down after inhibition of mitotic spindle function (21), (*iii*) no NE breakdown can be seen around the site of TPPP/p25 injection in cleavage *Drosophila* embryos.

The discrepancy between complete lack of NE disassembly in *Drosophila* after TPPP/p25 injection vs. only delay in NE disassembly after nocodazole treatment in mammalian cells (21) can be explained by the timing of the processes. Nocodazole delays NE disassembly by ≈8 min in mammalian cells. Such a delay in NE disassembly would lead to complete lack of NE disassembly during the cleavage division in *Drosophila* because the whole mitotic wave takes ≈6 min at 20°C in this system.

GTP Counteracts with TPPP/p25 in *Drosophila* Embryos. To demonstrate TPPP/p25 interaction with GTP *in vivo*, we coinjected TPPP/p25 with ≈60-fold excess of GTP into cleavage *Drosophila* embryos expressing tubulin–GFP fusion protein. (Higher GTP concentrations cause NE assembly defects.) During the next mitotic wave (from 15 min after injection), mitotic spindles form in the whole embryo (see Fig. 5 *A* and *B*), even around the site of injection, showing that GTP eliminates the inhibitory effect of TPPP/p25 on mitotic spindle formation. Chromatin segregation and NE reassembly seems to be unaffected, too, because the number, size, shape, and distribution of nuclei are completely normal in the next interphase (Fig. 5*C*). The coinjection experiment revealed that GTP interferes with the TPPP/p25-induced effects *in vivo*, similarly to that observed in the *in vitro* experiments that showed that GTP inhibits the TPPP/p25-induced tubulin assemblies (see Fig. 2*B*). During the second mitotic wave after injection (from 30 min after injection), mitotic spindles form (Fig. 5*D*) and nuclei are doubled (Fig. 5*E*) in number only at the anterior (control) part of the embryo. Apparently, 30 min are sufficient for the embryo to metabolize the excess GTP injected, and thus TPPP/p25 can exert its deleterious effect on mitotic spindle formation.

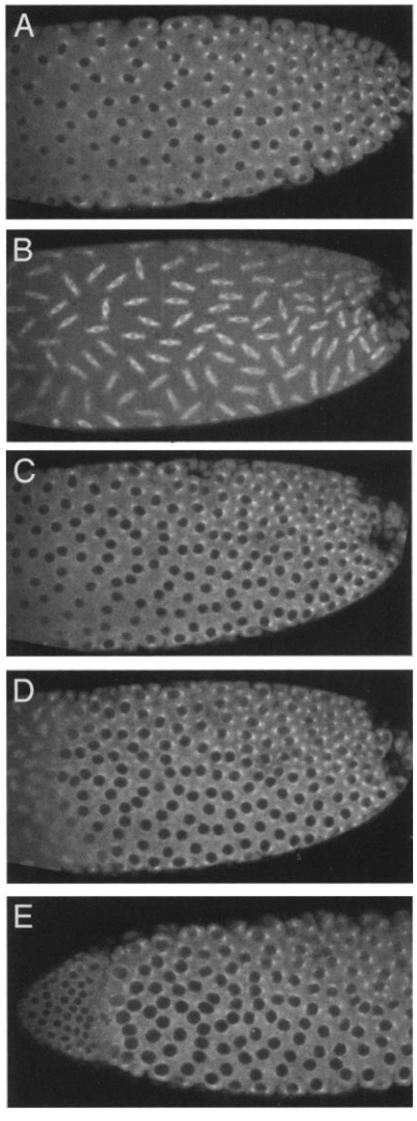

Fig. 5. GTP abolishes the effect of p25 on mitotic spindle formation. p25 was coinjected with GTP into the posterior pole of a tubulin–GFP-expressing cleavage *Drosophila* embryo. In the first interphase after injection, nuclei seem normal (*A*). During the next mitotic wave, mitotic spindles form normally in the whole embryo, indicating that p25 cannot exert its effect in the presence of GTP (*B*). After breakdown of the mitotic spindles, nuclei form normally in the whole embryo (*C*). During the second mitotic wave after p25 injection, mitotic spindles form and NE breaks down only in the anterior part of the embryo (*D*). In the upcoming interphase, the embryo contains normal-sized nuclei at the anterior tip whereas nuclei in the remaining part of the embryo are larger because they failed to divide.

Discussion

TPPP/p25/p24 was originally found in the partially purified fraction of bovine tau kinase II (7) and in the partially purified fraction of glycogen synthase kinase-3 (10). The function of the protein was unknown. Working with extracts from different tissues, we recognized that brain and neuroblastoma, but not muscle extracts, contain protein factor(s) that perturb the MT assembly induced by addition of paclitaxel (19). This protein factor was isolated from bovine brain, purified to homogeneity, and identified by information-dependent-acquisition liquid chromatography/mass spectrometry as a brain-specific protein, p25 (6). Based on its effect on tubulin polymerization, we denoted it as TPPP/p25 tubulin polymerization-promoting protein.

The results obtained by searching the homology at amino acid and nucleic acid levels suggest that the bovine TPPP/p25 protein is a member of a new protein family, characterized by high homology of C-terminal parts of the sequences. The only protein of the family isolated and characterized so far is bovine TPPP/p25. Sequence analysis suggests that the identity between bovine and human TPPP/p25 proteins is very high (90%) (compare Fig. 6), which increases the impact of our data obtained by bovine protein.

The most important finding of our experiments is that tubulin is a molecular target of TPPP/p25 and their interaction has an impact on the organization of the microtubular network both *in vitro* and *in vivo*. We have demonstrated that, under *in vitro* conditions, TPPP/p25 induces aberrant tubulin assembly due to substoichiometric binding of TPPP/p25 with tubulin. The dissociation constant of the tubulin-TPPP/p25 complex as determined by SPR experiments is 0.2 μM. This value is lower as found for interaction of tubulin and other cytosolic proteins (22). The cytoplasmic concentration of this protein estimated on the bases of yield of isolation is roughly 0.1 μM. However, TPPP/p25

is unevenly distributed in the brain (23); therefore, it might be expected that, in the cells in which it is present, a significant fraction of TPPP/p25 is associated with the MT network *in vivo*.

Injection of bovine-derived TPPP/p25 into cleavage *Drosophila* embryos expressing tubulin–GFP fusion protein allowed us to investigate the *in vivo* effect of TPPP/p25 on cellular events in more details. In agreement with data obtained *in vitro*, the injection experiments revealed that TPPP/p25 targets the microtubular network manifested by its inhibitory effect on the formation of mitotic spindles. We demonstrate that TPPP/p25 functions as a modulator of dynamics of microtubular network due to its binding to tubulin. The molecular mechanism of this phenomenon needs further studies. Based on *in vitro* observation, we speculate that TPPP/p25 may stimulate the formation of nonphysiological tubulin assemblies, thereby restricting the growth of conventional MTs. The *in vivo* observations that the much more dynamic mitotic MTs seem to be more sensitive to TPPP/p25 than the interphase MTs [i.e., that mitotic spindle formation is completely blocked by TPPP/p25, but that nucleation of MTs by centrosomes, their microtubular-based segregation, and the size of interphase MT asters (particularly evident on Fig. 5 *D* and *E*) are largely unaffected] are in line with a mechanism that TPPP/p25 "titrates free tubulin away".

An important factor that does modulate the interaction of TPPP/p25 with tubulin is GTP. GTP is present in brain tissue and is a key regulatory ligand of MT assembly by its binding to specific sites of tubulin. We found that GTP inhibits the binding of TPPP/p25 to tubulin (compare Fig. 2) at a concentration comparable with that observed *in vitro* and counteracts the inhibitory effect of this protein on the formation of mitotic spindle when coinjected with TPPP/p25 into cleavage *Drosophila* embryos. This result demonstrates that the counteracting effect of GTP on the changes induced by TPPP/p25 in the microtubular network is manifested under *in vivo* condition as well.

Another factor that may influence the binding/function of TPPP/p25 in brain system is the presence of other cytosolic proteins the binding of which has been extensively demonstrated *in vitro*. In fact, we have observed that, when the assembly of endogenous tubulin of cell-free brain extract has taken place, the highly decorated MTs appeared as intact tubules (24).

Our additional results show that TPPP/p25 injected into *Drosophila* embryos expressing tubulin–GFP specifically interferes not only with mitotic spindle formation but with NE breakdown as well. Recently, spindle-MT and the MT-associated motor cytoplasmic dynein were shown to facilitate NE breakdown during mitosis by tearing of the nuclear lamina (21, 25). MTs act as a mechanical checkpoint at prometaphase, coupling mitotic spindle assembly and NE breakdown. If so, the inhibition of spindle assembly by TPPP/p25 offers a plausible explanation for the failure of NE breakdown in the injected embryos.

Although TPPP/p25 very effectively interferes with mitotic spindle assembly, TPPP/p25 does not block replication and the MT-dependent separation of the daughter centrosomes. The centrosomes in the TPPP/p25-affected region nucleate just as nice MT asters as the centrosomes in areas from which TPPP/p25 is absent because centrosomes show the same fluorescence intensity in both areas of tubulin–GFP embryos. The above finding suggests that TPPP/p25 specifically blocks the formation of mitotic spindles without any dramatic interference on other MT dependent functions.

Immunohistochemistry revealed the localization and association of TPPP/p25 with oligodendrocytes, neuropil, and some unidentified fiber-like structures in the hippocampal regions of rat brain. The protein was reported to be only slightly expressed during the embryonic period in rat brain; its expression increased extensively in the first weeks after birth, then gradually increased until 1–2 years of age (23). This expression pattern of TPPP/p25 supports a hypothesis that TPPP/p25 might play a physiological role during cell differentiation; another possible function of TPPP/p25 might be the stabilization of microtubular bundles in axons. On the other hand, our findings that this protein induces the formation of tubulin aggregates and of nonphysiological microtubular superstructures *in vitro* suggest that TPPP/p25 (when overexpressed or when the GTP level is lowered) may play a role in neurodegenerative processes.

We thank Prof. S. Hollán and G. Timinszky for critical reading of the manuscript. This work was supported by Hungarian National Scientific Research Fund Grants OTKA T-031892 and B-044730 (to J. Ovádi), T-029924 and T-035019 (to F.O.), and T-032540 and T-043158 (to J.S.), and Hungarian Ministry of Education Grants NKFP-1/047/2001 MediChem and OMFB-00701/2003 (to J. Ovádi) and OMFB-00703/2003 (to J.K.). L.T. is the recipient of a Bekesy Fellowship.

1. Desai, A. & Mitchison, T. J. (1997) *Annu. Rev. Cell Dev. Biol.* **13,** 83–117.
2. Nogales, E. (2000) *Annu. Rev. Biochem.* **69,** 277–302.
3. Orosz, F., Santamaría, B., Ovádi, J. & Aragón, J. J. (1999) *Biochemistry* **38,** 1857–1865.
4. Vértessy, G. B., Bánkfalvi, D., Kovács, J., Lőw, P., Lehotzky, A. & Ovádi, J. (1999) *Biochem. Biophys. Res. Comm.* **254,** 430–435.
5. Kovács, J., Lőw, P., Pácz, A., Horváth, I., Oláh, J. & Ovádi, J. (2003) *J. Biol. Chem.* **278,** 7126–7130.
6. Hlavanda, E., Kovács, J., Oláh, J., Orosz, F., Medzihradszky, K. F. & Ovádi, J. (2002) *Biochemistry* **47,** 8657–8664.
7. Takahashi, M., Tomizawa, K., Ishiguro, K., Sato, K., Omori, A., Sato, S., Shiratsuchi, A., Uchida, T. & Imahori, K. (1991) *FEBS Lett.* **289,** 37–43.
8. Shiratsuchi, A., Sato, S., Oomori, A., Ishiguro, K., Uchida, T. & Imahori, K. (1995) *Biochem. Biophys. Acta* **1251,** 66–68.
9. Seki, N., Hattori, A., Sugano, S., Suzuki, Y., Nakagawara, A., Muramatsu, M., Hori, T. & Saito, T. (1999) *J. Hum. Genet.* **44,** 121–122.
10. Martin, C. P., Vazquez, J., Avila, J. & Moreno, F. (2002) *Biochim. Biophys. Acta* **1586,** 113–122.
11. Patrick, G. N., Zukerberg, L., Nikolic, M., de la Monte, S., Dikkes, P. & Tsai, L.-H. (1999) *Nature* **402,** 615–622.
12. Bradford, M. M. (1976) *Anal. Biochem.* **72,** 248–254.
13. Na, C. N. & Timasheff, S. N. (1986) *Biochemistry* **25,** 6214–6222.
14. Liliom, K., Wágner, G., Pácz, A., Cascante, M., Kovács, J. & Ovádi, J. (2000) *Eur. J. Biochem.* **267,** 4731–4739.
15. Grieder, N. C., de Cuevas, M. & Spradling, A. C. (2000) *Development* **127,** 4253–4264.
16. Gish, W. (1996–2003) BLASTP (Washington University, St. Louis, MO), http://blast.wustl.edu, Version 2.0.
17. Zhang, Z., Wu, C., Huang, W., Wang, S., Zhao, E., Huang, Q., Xie, Y. & Mao, Y. (2002) *J. Hum. Genet.* **47,** 266–268.
18. Kemp, B. E. & Pearson, R. B. (1990) *Trends Biochem. Sci.* **15,** 342–346.
19. Liliom, K., Wágner, G., Kovács, J., Comin, B., Cascante, M., Orosz, F. & Ovádi, J. (1999) *Biochem. Biophys. Res. Commun.* **264,** 605–610.
20. Lehotzky, A., Pálfia, Z., Kovács, J., Molnár, A. & Ovádi, J. (1994) *Biochem. Biophys. Res. Commun.* **204,** 585–591.
21. Beaudouin, J., Gerlich, D., Daigle, N., Eils, R. & Ellenberg, J. (2002) *Cell* **108,** 83–96.
22. Ovádi, J. & Orosz, F. (1996) in *Channelling in Intermediary Metabolism*, eds. Agius, L. & Sherratt, H. S. A. (Portland Press, London), pp. 237–268.
23. Takahashi, M., Tomizawa, K., Fujita, S. C., Sato, K., Uchida, T. & Imahori, K. (1993) *J. Neurochem.* **60,** 228–235.
24. Orosz, F., Wágner, G., Liliom, K., Kovács, J., Baróti, K., Horányi, M., Farkas, T., Hollán, S. & Ovádi, J. (2000) *Proc. Natl. Acad. Sci. USA* **97,** 1026–1031.
25. Salina, D., Bodoor, K., Eckley, D. M., Schroer, T. A., Rattner, J. B. & Burke, B. (2002) *Cell* **108,** 97–107.